



Simulation and Modeling for Aging and Particle Shape Effect on Airflow Dynamics and Filtration Efficiency of Human Lung

J. Kori[†] and Pratibha

Department of Mathematics, Indian Institute of Technology Roorkee, Roorkee, Uttarakhand, 247667, India

[†]Corresponding Author Email: [jyotikori@gmail.com](mailto: jyotikori@gmail.com), [kjyoti@ma.iitr.ac.in](mailto: kjyoti@ma.iitr.ac.in)

(Received June 19, 2018; accepted October 31, 2018)

ABSTRACT

The respiratory system undergoes various physiological and immunological changes with age. After birth, alveolization is one of the main factor associated with progressive growth of lung, which is relatively poorly analysed in respect of lung function. In this study we considered growth of lung caused by progressive increment in number of alveoli and simultaneously calculated its effect on airflow dynamics and filtration efficiency of human lung from childhood to age of 30. Incorporating the idea of filtration through lung with respect to age biofilter model is used by assuming porosity of lung varied with respect to number of alveoli and their surface area. Transportation and deposition properties of nanoparticles of various shapes during inhalation is taken under consideration by using particle shape factor. Generalized Navier Stokes equation is used for flow dynamics and finite difference scheme is used to solve the problem numerically. Simulation is done by using user defined code on MATLAB at very fine grid. Results indicate that the filtration efficiency of lung decreases as age increases from childhood to age of 30; additionally, nonspherical nanoparticles with high aspect ratio's will take a longer time to be filtered from lung as compared to spherical nanoparticles of the same diameter.

Keywords: Aging; Alveolar region; Filtration efficiency; Growth of lung; Lung function; Nanoparticle; Porosity.

NOMENCLATURE

a	radius of duct	S'	surface area of nonspherical particle
b_l	biological degradation constant	S	surface area of spherical particle
C	Cunningham slip correction factor	s_f	shape factor
d	diameter of spherical particle	S_f	dynamic shape factor
Da	Darcy number	S_k	Stockeian coefficient
D_p	aerodynamic diameter of nonspherical particle	$S_{ }$	parallel orientation of particle
E	porosity of media	S_{\perp}	perpendicular orientation of particle
F	drag force on spherical particle	T	time
F_d	drag force on nonspherical particle	t'	dimensionless traveling time
K	permeability	Ua	velocity of air flow
K_m	partitioning coefficient	V_p	velocity of dust particles
m	mass of dust particle	z	radial axis
N_a	number of alveoli in human lung	β	particle aspect ratio
N_d	number density of the dust particles	ρ_0	unit density
P	fluid pressure	ρ	density of air
P_0	atmospheric pressure	ν	effective viscosity parameter
r	axial axis	μ	coefficient of dynamic viscosity of air
R	breathing rate	λ	mean free path of the gas
r'	radius of lung		
r_o	radius of alveoli		

1. INTRODUCTION

Nanoparticles are very small size particles, which can be considered as a subcategory of ultrafine

particles (Laurent *et al.* 2010) and found in agriculture, coal mines, incomplete combustion of diesel engines, organic fragments and fine hairs from plants and animals, grinding and polishing processes,

atmospheric dust, industry of cosmetic, cloth, furniture, material etc.. However, nanoparticles are also produced by several kinds of indoor activities such as smoking, cooking, candle-burning or other combustion related processes. These particles are sub divided with respect to their dimensions such as zero, one, two and three (Tiwari *et al.* 2012) and named as nanodots, nanowires, nanotubes, quantum crystals (Aitken *et al.* 2004) etc.. One of the most prominent and notorious nanoparticle is fiber, which is an exposure of different kind of asbestos and found to be curly and irregular in shape such as stretched spheroid, elongated or oblate. These fibers are responsible for occupational hazard, which increases the incidence of lung cancer for asbestos workers because these kind of particles have a large probability of reaching in the vulnerable gas exchange region in deep lung; one of the best example of this range is multi-walled carbon nanotubes (Hogberg *et al.* 2010). The structure and dimensions of airways, tidal volume of lung, breathing frequency, fiber shape and size etc. (Asgarian & Ahmadi 1998) are the most prominent parameters, which are responsible for penetration and deposition of these kind of dust particles in various generation (0-23, trachea to alveoli) of lung.

There are various studies (Dunnill, 1962; Xu & Yu 1986, Menache & Graham 1997) which suggested that the deposition of particles as well as human lung architecture and tissue parameters vary with respect to age.

Age is allied to the development of lung. In 1970 Davies and Reid (1970) give age based study of human alveoli, in which he stated that number of alveoli is closely related to total lung volume with larger lungs having considerably more alveoli. Alison and Lynne (1974) suggested that during birth 24 mil-lion alveoli are present, and by the age of 8 years this was increased to 300 million. By using design-based stereologic approach Ochs *et al.* (2004) calculated the mean alveolar number was 480 million. So, reconstruction would seem to indicate that development of lung is due to increment in number of alveoli along with alveolar ducts. Moreover, viscoelastic porous nature of human lung is by virtue of alveoli along with a dense network of blood capillaries (pulmonary parenchyma) (Pozin, 2017). By using computational fluid dynamics DeGroot and Straatman (2018) developed a porous media based approach based on the theory of volume-averaging by considering the small scale airways and alveoli as a porous domain. Author predicted permeability of media caused by expansion and contraction of alveoli. Consequently, for structural determinant of lung architecture number of alveoli, which are vary with age, is a key parameter Emery and Mithal (1960).

Moreover, aging causes variation in respiratory condition, due to which accurate information of aerosol deposition and clearance in the growing lung is critical not only for infants and children, but also in adults. According to Hofmann (1982) total deposition within the human lung decreased with increasing age from 7 months to 30 years. In 2016 Sturm (2016) presented a work on deposition of

bioaerosols with various shapes and sizes in the tracheobronchial tree of probands with different ages (1-20 yr) and stated that bioparticles have higher possibility to reach and deposit the alveoli in adults than infant's and children's and deposition of bioparticle is correlated positively with age. In the same year a numerical prediction was made in support with vivo findings by Behnke *et al.* (2012) given by Henry and Tsuda (2016) on postnatal development and particle deposition. According to their study, in humans, major structural change occurs over the first 2 yrs of life and during this post-natal development the shape of alveolar affects the rate of deposition of nanoparticles deep in the lung.

Svartengren *et al.* (2005) observed 46 healthy subjects from 19-81 yrs and stated that clearance over 21 days was decreased with age. Sturm (2014) simulated clearance of single and multi walled carbon nanotubes by using a mathematical approach and found that single walled carbon nanotubes reside significantly longer in the lungs than multi walled carbon nanotubes because for single walled carbon nanotubes, mucociliary clearance takes 24 h after exposure, slow bronchial clearance takes half-time of 5 d, whereas alveolar clearance takes half-times >100 d compared to multi walled carbon nanotubes. Additionally, he concluded that long single walled carbon nanotubes have a higher probability of alveolar deposition than multi walled carbon nanotubes. Saini *et al.* (2015) modeled alveolar sacs as a biofilter with constant porosity to filter inhaled spherical nanoparticles and concluded that high removal efficiency require large amount of traveling time. Roman *et al.* (2016) found that between the ages of 25-80 years pulmonary function and aerobic capacity decline by 40%. In 2017, Sturm (2017) presented age (1-20 year) based theoretical study for clearance biogenic particle and concluded that very fine (<0.01 μ m) particles cost highest clearance rates than very coarse particles (>5 μ m) (preferentially deposited in the up-per bronchial airways), whilst large particles takes several months to years to remove due to their accumulation in the alveoli.

From literature review we found there are various theoretical and experimental studies who stated effect of aging on particle deposition, clearance and lung structure, whereas there are only a few mathematical studies which observed effect of nanoparticle deposition and clearance with respect to aging. By considering lung as a variable porous media and calculate its filtration efficiency by using biofilter model to remove inhaled nonspherical nanoparticle with respect to aging is still unsolved. The motivation behind this study is comprehend the effect of age on filtration efficiency of lung. For this purpose, we used a generalized Navier-Stokes equation for flow dynamics of viscous air through lung, which is a variable porous media. We chose number of alveoli is a key factor changes with age from childhood to adult and responsible for porous behavior of lung. Also, particle shape factor is used to quantify the deposition and clearance of various shape nanoparticles by using biofilter model with respect to age. Finite difference numerical method is used to get simple discretized equations and com-

putational work is performed by using user defined code on MATLAB R2016, 126 GB RAM workstation for very fine grid. The effect of various flow governing parameters (aspect ratio, Darcy number, porosity) on the flow and filtration efficiency have been investigated in addition to a comparison with published work (Saini et al. 2015).

2. MATHEMATICAL MODEL

2.1 Physical Configuration

The physical model of the present problem is shown in Fig. 1. Figure 1a is the architecture of the tracheo-bronchial tree and the pulmonary region (Sturm & Hofmann 2009) and Fig. 1b is the simplified model of alveolar region, through which viscous air is flowing. Radius of duct is 'a', and attached terminal alveoli is 'r₀'. Dirt can be accumulated either on the sides and turns of the ducts or inside alveolies, which can be filtered by the mechanism of mucociliary clearance or coughing. Consequently, we considered alveolar or pulmonary region as a biofilter media.

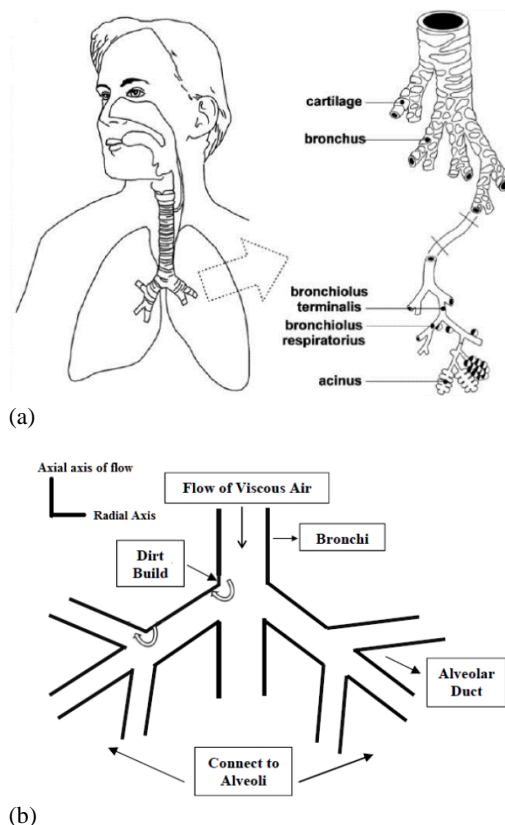


Fig. 1. (a) Architecture of the tracheobronchial tree and the alveolar region (b) Simplified model of alveolar region for viscous air flow.

2.2 Governing Equations

An incompressible fully-developed steady laminar and Newtonian fluid is flowing along the axis of the tube with no slip boundary condition and time dependent sinusoidal pressure gradient. We approximate airways or alveolar duct as a circular

cylinder and flow of viscous fluid is along the axis of the tube only; therefore, one dimensional cylindrical polar coordinate system (r, t) is used to ease the problem. A mathematical model proposed by Yan et al. (2008) and used by Saini et al. (2015) is taken under consideration after including variable porosity and particle shape factor terms to find the filtration efficiency of lung at different ages (1-30 years). One dimensional flow governing equations that satisfies our assumptions are given below.

$$\nabla U_a = 0 \tag{1}$$

$$\frac{\partial U_a}{\partial T} + \frac{U_a}{E} \frac{\partial U_a}{\partial r} = -\frac{E}{\rho} \frac{\partial P}{\partial r} + \nu \left(\frac{\partial^2 U_a}{\partial r^2} + \frac{1}{r} \frac{\partial U_a}{\partial r} \right) + \left(-\frac{E\nu}{K} U_a + s_k \frac{N_d}{\rho} (V_p - U_a) \right) \tag{2}$$

Here, K denotes permeability, which was defined by Ergun (1952) in terms of porosity (E) of media as follows:

$$K = \frac{E^3 D_p^2}{150(1-E)^2} \tag{3}$$

According to Weibel (1963) each of the structural components such as airways, alveoli, and blood vessels has different growth patterns in number as well as in size. After using Weibel model, Hofmann (1982) defined an age dependent lung geometry from birth to adulthood in which the total number of alveoli N_a increases with age as follows:

$$N_a = [37.6 + (1 - e^{-0.4\tau}) 286.21] 10^6, \tag{4}$$

$$\tau = 1, 2, \dots, 30 \text{ year}$$

Alveolies inside the lung are the void spaces, which can be approximated as spherical bubble and responsible for porousness and growth of lung (De-Groot and Straatman (2018)). Moreover there are theoretical, experimental and vivo studies (Dunnill, 1962, Quirk et al. 2016, Kim et al. 2017) which stated that not only number of alveoli but their surface area also are linearly associated with aging. So, by using equation (4) we modeled lung as a porous media and its porosity (E) can be de-fined combinedly by product of number of alveoli and ratio of surface area of single alveoli to total surface area of lung as follows,

$$E \approx N_a \left(\frac{r_0}{r} \right)^2 \tag{5}$$

Additionally, to analyse the filtration/clearance efficiency of lung the property of nanoparticles such as size and shape (Jiang et al. 2000) are also very important factors. There are different models in which size dependent properties have been explained, some models assumed nanoparticles as ideal spheres (Nanda et al. 2002) while others worked on polyhedral, disk like nanoparticles (Simakin et al. 2001). Nanoparticle shape factor sf is defined as the ratio of the surface area of a nonspherical nanoparticle (S') to the surface area of spherical nanoparticle (S), where both of the nanoparticle have identical volume (Qi et al. 2005),

$$s_f = \frac{S'}{S} \tag{6}$$

Generally, for polyhedral shape, nanoparticle surface is composed of different planes. So, the surface area of a nanoparticle is the sum of all area of the planes,

$$S' = \sum_i S_i \tag{7}$$

Where, S_i is the area of the plane i . However, [Sturm and Hofmann \(2009\)](#) mentioned the concept of particle orientation in their study. The particle shape factor is renamed as dynamic shape factor (S_f) ([Stober, 1972](#)) and can be written in terms of particle orientation as follows:

$$S_f = \frac{1}{3} \left[\frac{1}{S_{\perp}} + \frac{2}{S_{\parallel}} \right] \tag{8}$$

In Eq. (8) S_{\parallel} represents parallel orientation of particles and S_{\perp} represents perpendicular orientation of particles with respect to the direction of flow. Both factors are defined by the following equations for elongated or prolate particles as below,

$$\left. \begin{aligned} S_{\perp} &= \frac{\frac{8}{3}(\beta^2 - 1)\beta^{-\frac{1}{3}}}{\left(\frac{2\beta^2 - 3}{1}\right)\ln(\beta + (\beta^2 - 1)^{\frac{1}{2}}) + \beta} \\ S_{\parallel} &= \frac{\frac{4}{3}(\beta^2 - 1)\beta^{-\frac{1}{3}}}{\left(\frac{2\beta^2 - 1}{1}\right)\ln(\beta + (\beta^2 - 1)^{\frac{1}{2}}) - \beta} \end{aligned} \right\} \beta > 1 \tag{9}$$

Where, β is the aspect ratio of particle length to particle width. For extremely long fibers, $\beta \gg 1$ and for extremely thin disks, $\beta \ll 1$. In the case of oblate particle geometries, the following equations are commonly used,

$$\left. \begin{aligned} S_{\perp} &= \frac{\frac{8}{3}(\beta^2 - 1)\beta^{-\frac{1}{3}}}{\left(\frac{2\beta^2 - 3}{1}\right)\arccos \beta + \beta} \\ S_{\parallel} &= \frac{\frac{4}{3}(\beta^2 - 1)\beta^{-\frac{1}{3}}}{\left(\frac{2\beta^2 - 1}{1}\right)\arccos \beta - \beta} \end{aligned} \right\} \beta < 1 \tag{10}$$

As demonstrated above, Eq. (9) only differs from Eq. (10) insofar as the natural logarithm is substituted by an arcuscosinus function. In terms of drag force the dynamic shape factor can be described as the ratio of the drag force, of the nonspherical nanoparticle (F_d) to the drag force (F) of the equivalent spherical particle with the same volume ([Hinds, 1999](#)).

$$S_f = \frac{F_d}{F} \tag{11}$$

We used the following equation for velocity of non-spherical particles through duct,

$$m \frac{\partial V_p}{\partial T} = F_d \tag{12}$$

$F = sk(Ua - Vp)$, where $sk = 3\pi\mu D_p/C$ is the Stokes resistance coefficient for spherical particles and C , Cunningham slip correction factor is used for free molecular flow regime.

$$C = 1 - \frac{\lambda}{D_p} \left[2.514 + 0.800 \exp\left(\frac{-0.55D_p}{\lambda}\right) \right] \tag{13}$$

In continuation, the aerodynamic diameter determines how well the particles enter and how far they go in the lungs. Nonspherical nanoparticle geometries are most reliably approximated with the help of the aerodynamic diameter

(D_p), which was de-fined by [Stober \(1972\)](#) as follows.

$$D_p = d \sqrt{\frac{\rho}{S_f \rho_0}} \tag{14}$$

In Eq. (2) the pressure gradient due to periodic breathing rate (R) takes the following form:

$$-\frac{\partial P}{\partial r} = P_0 \sin(\pi RT) + S_f \tag{15}$$

2.3 Assumptions

To solve the mathematical model following assumptions are made.

1. The optimal particle size is nano and particle shape is nonspherical; preferably elongated.
2. Assuming that the particles are homogeneously distributed throughout the inhaled volume and all deposition occurs during in-halation.
3. Variable porosity of lung and shape factor of nonspherical nanoparticles are assumed to analyse the filtration behavior of lung.
4. The number of alveoli is assumed to be a function of time (in years) and porosity is a function of number of alveoli or therefore, porosity is a function of time (in years).

2.4 Initial Conditions

Initial conditions for $T \leq 0, 0 \leq r \leq 1$ are as follows:

$$U_a(r,T) = V_p(r,T) = \left(\frac{\partial U_a}{\partial r}\right)_{r,T} = 0 \tag{16}$$

2.5 Boundary Conditions

The no slip boundary conditions are used due to pulmonary surfactant at $T > 0$ and $r=0$ & a .

$$\begin{aligned} U_a(r,T) &= 0 \\ V_p(r,T) &= 0 \end{aligned} \tag{17}$$

3. METHODOLOGY

3.1 Transformation of the Governing Equations

To solve the equations numerically we have to make above equations dimensionless by using following quantities.

$$z^* = \frac{r}{a}, p^* = \frac{Pa^2}{\rho v^2}, t^* = \frac{Tv}{a^2}, u^* = \frac{aU_a}{v}, v^* = \frac{aV_p}{v} \tag{18}$$

After dropping the asterisk (*) the above equations are written as follows:

$$\frac{\partial u}{\partial t} + \frac{u}{E} \frac{\partial u}{\partial z} = -E \frac{\partial p}{\partial z} + \left(\frac{\partial^2 u}{\partial z^2} + \frac{1}{z} \frac{\partial u}{\partial z} \right) + B(v-u) - \frac{E}{Da} u \tag{19}$$

$$\frac{\partial v}{\partial t} = \frac{S_f(u-v)}{t} \tag{20}$$

Here, Da is Darcy number and B, M, t are used for simplification.

3.2 Numerical Method

The finite difference, a basic and less cumbersome technique for regular geometries (Smith, 1985, Kori & Pratibha 2018, Saini et al. 2015) is used to solve the transformed governing equations.

3.2.1 Discretization of the Components

The discretization of velocity, u (z, t) is written as u(z_i,t_j) or u_{i,j}, when grid space and time steps are chosen as follows:

$$\begin{aligned} z_i &= i \Delta z; i = 0, 1, 2, 3, \dots, N, z_N = 1.0 \\ t_j &= (j - 1) \Delta t; j = 1, 2, \dots \end{aligned} \tag{21}$$

where i and j are the space and time indexes, and Δz and Δt are the increment in axial direction and time respectively.

We used central difference approximations for all the spatial, and second order time and space derivatives, and forward difference approximation for first order time derivative at point (z_i,t_j) as defined below:

$$\begin{aligned} \frac{\partial u}{\partial z} &= \frac{u_{i+1,j} - u_{i-1,j}}{2\Delta z} \\ \frac{\partial^2 u}{\partial z^2} &= \frac{u_{i+1,j} - 2u_{i,j} + u_{i-1,j}}{(\Delta z)^2} \\ \frac{\partial u}{\partial t} &= \frac{u_{i,j+1} - u_{i,j}}{\Delta t} \end{aligned} \tag{22}$$

After applying above mentioned discretization technique we got velocity profiles at the (j + 1)th time level in terms of the velocity at jth time level for Equations (19) and (20) respectively.

All the symbols used in this study are already defined in the nomenclature section.

3.2.2 Stability Criteria

To calculate the flow dynamics and filtration behavior of lung, a code is developed on MATLAB R2016 and mesh dependency of the solution was inspected for Δz ≤ 0.0014 and Δt ≤ 10⁻⁶, but result remains consistent for Δz = 0.01 and Δt ≤ 10⁻⁵, in the axial and radial directions. In this manner, entire calculations are done by taking the very fine grid size 100x100000 uniformly and we found that the result appeared to converge with the accuracy of order 10⁻⁵ by using following stability criteria.

$$\max \left\{ \frac{\Delta t}{\Delta z^2} \right\} \leq 0.5 \tag{23}$$

3.2.3 Model Validation

Before discussing the analysis of the present problem a numerical code validation and predictive accuracy of the model are checked by comparing out-put data produced by present model with respective results generated by model of Saini et al. (2015) for air velocity at Da = 0.1, E=0.6, exponential pressure gradient and represented in Fig. 2 (see in Table 1). Saini et al. (2015) studied flow of viscous air through a circular tube (like capillaries of alveolar sacs) by considering lung as a biofilter media with constant porous media and exponential pressure gradient. Author calculated filtration of spherical particle of diameter = 100 nm with constant porosity = 0.6 of lung by using removal efficiency model (Hodge & Devanny, 1995). Fig. 2 shows variation in velocity of air with time in constant porous domain. We found that our numerical result is validated with their result up to 99%. So, we can say, our results is in excellent agreement with those of Saini et al. (2015).

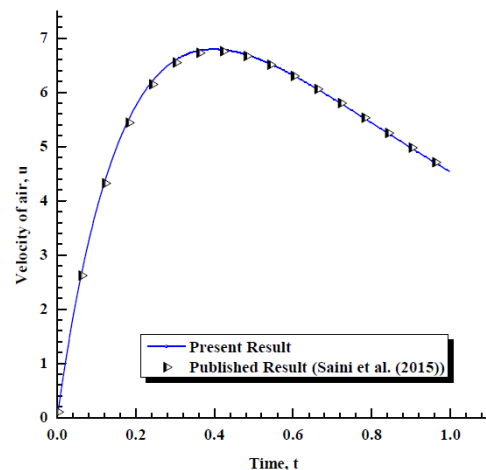


Fig. 2. Comparison between published (Saini et al. 2015) and present work for air velocity at Da = 0.1, d = 100nm and E = 0.6.

4. RESULTS AND DISCUSSIONS

In this work we aimed to find the effect of aging on flow dynamics and filtration efficiency of lung. To

Table 1 Comparison between published (Saini et al. 2015) and present result

t	Air Velocity, u	
	Present Result	Published Result (Saini et al. (2015))
0.1	3.83	3.77
0.2	5.75	5.69
0.3	6.59	6.54
0.4	6.8	6.76
0.5	6.65	6.63
0.6	6.32	6.31
0.7	5.89	5.9
0.8	5.44	5.45
0.9	4.98	4.99
0.998	4.54	4.56

analyse this, we calculated the effect of aspect ratio (b), orientation with respect to flow stream, aerodynamic diameter (D_p) of nonspherical nanoparticle together with effect of variable porosity (E) and Darcy number ($10^{-1} \leq Da \leq 10^{-3}$) on air pressure and flow dynamics. We also observed the effect of particle shape and variable porosity on the filtration efficiency of human lung with respect to age. Simulation was carried out by using numerical values defined in Table 2 & 3.

Table 2 Calculated shape factors for special shapes (Qi et al. 2005)

S.N.	Particle Shape	Shape factor (α)
1.	Spherical	1
2.	Regular tetrahedral	1.49
3.	Regular hexahedral	1.24
4.	Regular octahedral	1.18
5.	Disk-like	> 1.15

4.1 Effect of Aspect Ratio on Flow Dynamics

Velocity of fibrous particles is controlled by fiber aspect ratio (β). In this study we used regular octahedral, regular hexahedral, regular tetrahedral particles without orientation and prolate particles at $d = 50$ nm and $3 \leq \beta \leq 1000$ or disk shaped particles at $d = 50$ nm and $0:1 \leq \beta \leq 0:001$ with orientation effect. From Fig. 3b to Fig. 3c we can see the effect of various shapes and aspect ratios on the velocity of air and particles at age 15. We found, from Fig. 3a, velocity of regular tetrahedral particle is high as compared to octahedral particle, which causes decrease in the velocity of air for tetrahedral particles in Fig. 3b. Also due to increment in aspect ratio velocity of particle increases in Fig. 3c and velocity of air decreases in Fig. 3d with time. We can conclude by this, due to high aspect ratio, particles remain in air for a long time which cause a decrease in air velocity. As a consequence, nonspherical nanoparticle with high aspect ratio slow down the air flow and have more probability to trigger pro inflammatory effects and may reach and deposit deep inside lung.

4.2 Effect of Porosity on Flow Dynamics

According to Eq. (5), we noticed porosity of lung

vary from 0.2 to 0.7 due to age 1-30. To find the effect of porosity on flow dynamics we plotted time dependent graph of air and particles velocity at $\beta = 10$, $d = 50$ nm, $Da = 0.1$, which can be seen in Fig. 4a-4b. From these figures we found that porosity increases with increment in age (1 to 30 years), which causes increment in air and particle velocity with time. Consequently, we can say that the porous media with high porosity will allow air to flow more freely as compared to low porous media or physiologically we can say during childhood human lung is not enough porous to breath properly.

4.3 Effect of Particle Orientation on Flow Dynamics

In Fig. 5a and Fig. 5b we found the effect of different orientations of prolate particles for aspect ratio 10 and 1000 on the velocity of air and particle at the age = 15, $da = 0.1$ and $d = 50$ nm. From Fig. 5a and Fig. 5b we found that air and particle velocities increase in parallel orientation by increasing aspect ratio. However, air and particle velocity decrease in perpendicular orientation by increasing aspect ratio. Therefore, we can conclude that if particles are in parallel orientation then it may have tendency to go deep inside lung.

4.4 Effect of Darcy number on Air and Particle Velocity

Darcy number (Da) is very important for flow in porous media. We observed the effect of Da from 0.001 to 0.5 on flow dynamics at aspect ratio (β) = 10, $d = 50$ nm at age 15 in Fig. 6a and 6b. When Da decreases, velocity within the porous media decreases significantly. For small values of Da , the porous layer is considered less permeable for fluid penetration and fluid experiences pronouncedly large resistance as it flows through the porous matrix, which causes hindering the flow activities in the porous region. Additionally we found due to increment in Da , media pressure decreases and permeability increases; as a consequence, velocity of air and particle increases gradually with time by increasing value of Da .

4.5 Effect of Porosity on Pressure Gradient

A plot between pressure gradient and time with respect to age ($0.2 \leq E \leq 0.7$) is shown in Fig. 7. From

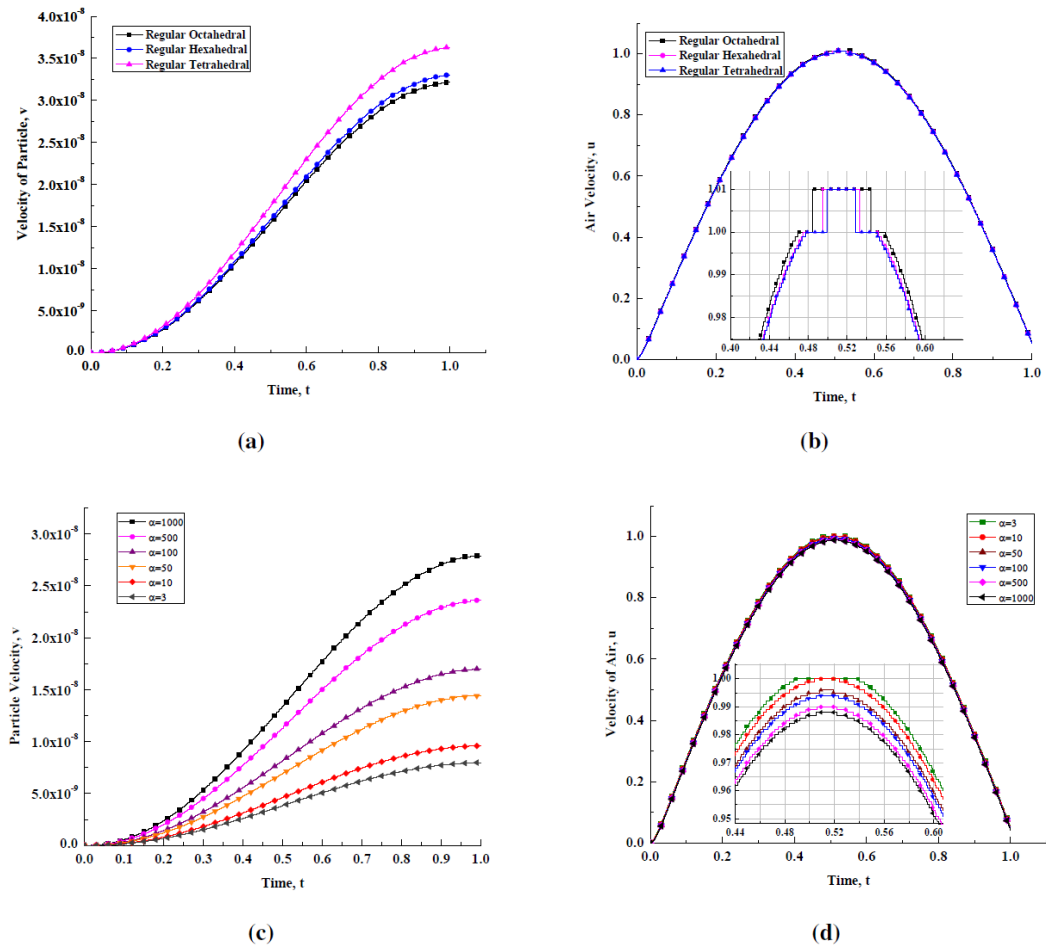


Fig. 3. Influence of shape factor without orientation of particle at age = 15 years (a) particle velocity, v (b) air velocity, u ; Influence of shape factor with orientation of particle at $3 \leq \beta \leq 1000$ and age = 15 years (c) particle velocity, v (d) air velocity, u .

Table 3 Values for numerical calculation

Variable	Value	Reference
a	$0.5 \mu m$	Saini et al. (2015)
ρ	$1.145 kg/m^3$	Saini et al. (2015)
ν	$1.52 \cdot 10^{-5} m^2/s$	Saini et al. (2015)
m	$0.0002 Kg/l$	Saini et al. (2015)
r_o	$0.11 mm$	
N_0	$0.02504 \cdot 10^{12}/m^3$	Saini et al. (2015)
d	$50 nm$	Rissler et al. (2017)
β	10-1000 and 0.1 to 0.001 for oblate	(Sturm 2015)
P_0	$101.325 k Pa$	Saini et al. (2015)
b_1	0.0061	Hodge and Devigny (1995)
ρ_0	$1kg/m^3$	
λ	$0.066 \mu m$	Sturm (2015)

this figure we found that pressure gradient decreases gradually with respect to age. For $E = 0.2868$ pressure is very high (for infant of 1 year), while for $E = 0.7037$ (for adult of 30 years), it is 142 Kpa. Accordingly, pressure will decrease as we increase media porosity.

4.6 Traveling Time and Filtration Efficiency of a Biofilter

In the biofilters, the traveling time of viscous air

passing through lung (porous media) is an important parameter to evaluate the filtration efficiency (F.E.). If the traveling time is too short, the biofilter cannot filter the deposited particles effectively, and if the traveling time is too long, the efficiency of biofilter would be too low. To calculate the traveling time, the porous media is divided uniformly into N nodes, and the path-lines passing through the N nodes are traced to determine the traveling time of each deposited particle. To analyse the performance of biofilter, one

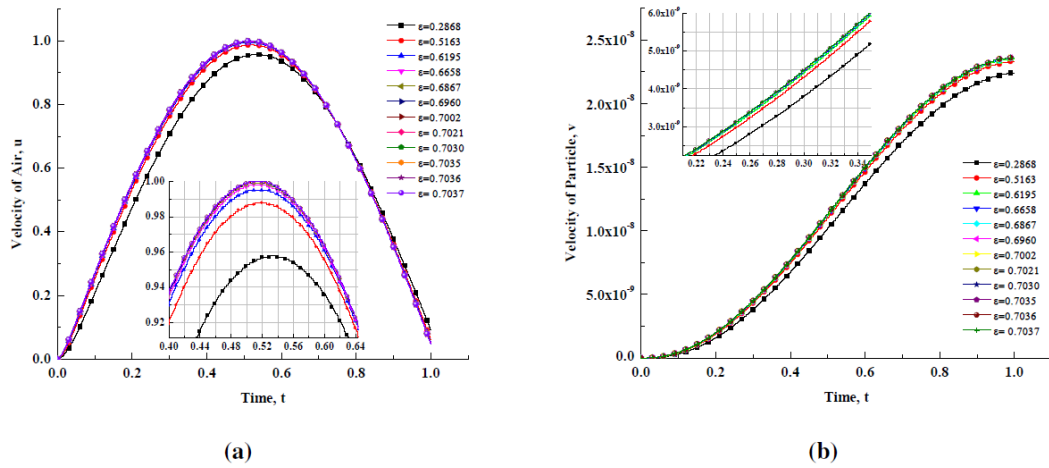


Fig. 4. Effect of lung porosity (obtained from age 1 to 30) on flow dynamics at $\beta = 10$, $d = 50$ nm, $Da = 0.1$ (a) air velocity, u and (b) particle velocity, v .

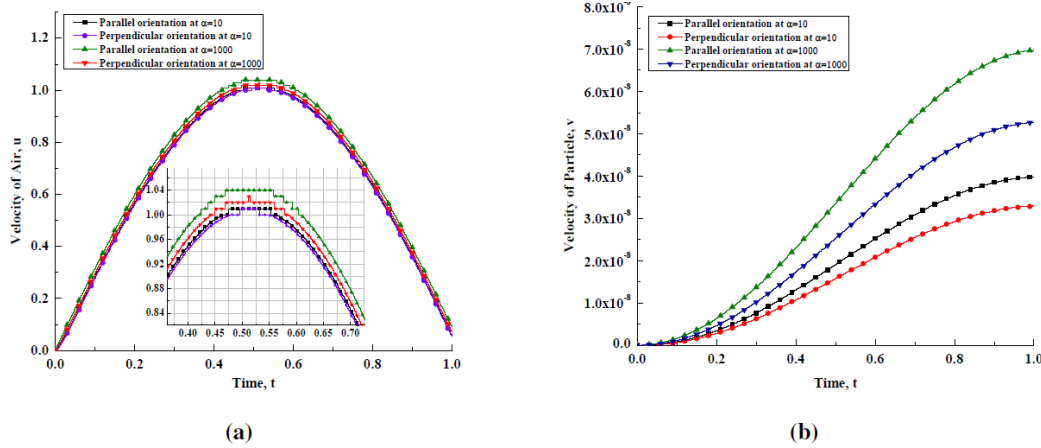


Fig. 5. Significance of parallel and perpendicular orientation of particle at $\beta = 10$ & 1000 on (a) air velocity u , and (b) particle velocity, v .

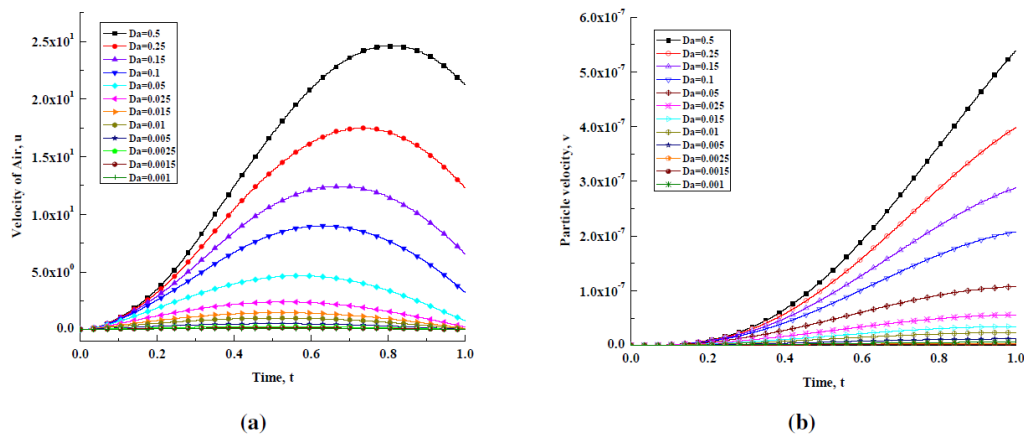


Fig. 6. Effect of Darcy number ($0.001 \leq Da \leq 0.5$) on flow dynamics at $\beta = 10$, $d = 50$ nm at age 15 (a) air velocity u , and (b) particle velocity, v .

of the main parameter is to find its efficiency. For this purpose we used a steady-state first-order degradation rate model, which can be defined (Hodge & Devanny, 1995, Yan, Su and Zhang, 2013, Saini *et al.* 2015) in dimensionless form as follows:

$$F.E. = 1 - \exp[-b_1 k_m t'] \tag{24}$$

Where, b_1 is biological degradation constant, k_m is partitioning coefficient and t' is dimensionless average traveling time of viscous air. The product of b_1 and k_m is constant and selected so that the

filtration efficiency was 90% at $\varepsilon = 0.9$, $Da = 10-3$. The time of travel of each particle was placed into Eq. (24) and the resultant F.E. were averaged. The average F.E. of the particles was taken as the total biofilter F.E. for that simulation. A more complete derivation of the F.E. model can be established in [Chitwood and Devanny \(1999\)](#).

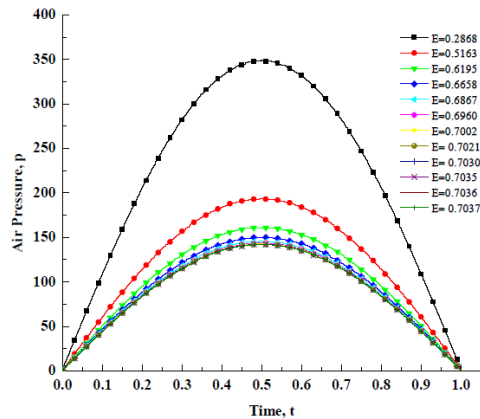


Fig. 7. Effect of porosity (0.2 E 0.7) with respect to age on air pressure.

4.6.1 Filtration Efficiency of Lung in Respect of Age

We aimed to find the F.E. of lung from age 1-30. For this purpose, we first calculated porosity of lung by Eq. (5) associated with age 3, 8, 13, 30 then the traveling time of each particle (being identical) and try to optimize above defined biofilter model at $\beta = 10$, $10^{(-1)} \leq Da \leq 10^{(-3)}$ in respect of age, as shown in Fig. 8a- 8d (Table 4). From these figures we can see, for particular age (3, 8, 13, 30) there is discernible variation in the F.E. and traveling time of particles. By decreasing Darcy number from 0.1 to 0.001, traveling time increases and F.E. decreases with respect to aging (from birth to age of 30). The results produced by present analysis are also compatible with the theoretical and physiological results by [Sturm \(2017\)](#) and can be useful to calculate F.E. of growing lung.

4.6.2 Filtration Efficiency of Lung in Respect of Shape Factor

In Fig. 9, we found F.E. of lung for spherical ($d=100\text{nm}$) and nonspherical nanoparticle ($10 \leq \beta \leq 1000$) by varying Darcy number $10^{(-1)} \leq Da \leq 10^{(-1)}$ in respect of age 15. For each graph we found at the same aspect ratio, the traveling time of particle increases when the Darcy number decreases from 0.1 to 0.001. As shown in Figs. 9a- 9e (Table 5), traveling time of particle and F.E. of lung increases by increasing β from 10 to 1000 and de-creasing Darcy number from 0.1 to 0.001. After analysis following observations can be made:

1. For spherical shape particles traveling time is less and it increases by increasing particle aspect ratio 10 to 1000.
2. High filtration efficiency cost large amount of

traveling time for nonspherical nanoparticle of aspect ratio 1000.

3. In Fig. 9e, for $Da=0.1$, we found F.E. of nonspherical nanoparticle of aspect ratio=1000 take much more traveling time as compared to spherical nanoparticle.

5. CONCLUSIONS

Human lung goes through various anatomical changes from birth to adulthood. Development of alveoli with age is one of the main factor of growth of lung. In this study we did age based study of nonspherical nanoparticle deposition and filtration of growing lung from age 1 to 30. For this purpose we model lung as a variable porous media and porosity depends on number of alveoli. In addition, we analysed efficiency of lung to filter nonspherical nanoparticle of different aspect ratio with diameter =50 nm. Effect of β , orientation of particle with respect to flow stream, Da , E are found graphically. The important results of the conducted study leads to the following conclusions.

1. In respect of shape factor velocity of particles related with this inequality, regular octahedral < regular hexahedral < regular tetrahedral and velocity of air related with this inequality, regular octahedral > regular hexahedral > regular tetrahedral.
2. It is noticed that air and particle velocity of elongated particles are affected by increasing their aspect ratio from 3 to 1000.
3. Due to parallel orientation of particles we found that the velocity of fluid increased.
4. By increasing Da from 0.001 to 0.1, velocity of fluid increased, which show by increasing Da pressure gradient decreases.
5. High porosity (during adulthood) reduces pressure gradient of lung.
6. It is found that the fraction of particles trapped in the alveolus increases by decreasing the Darcy number.
7. Due to aging, filtration efficiency of lung decreases and traveling time of particles increases.
8. Nonspherical nanoparticle of aspect ratio 1000 cost large amount of time to filter from lung as compare to spherical nanoparticle of the same diameter. By this we conclude, nonspherical nanoparticle with high aspect ratio have feasibility to hang in air stream and take longer time to deposit in deeper lung generations.

Finally, we found present results are compatible with published result ([Saini et al. 2015](#)) together with the physiology condition stated in theoretical and experimental studies of [Asgharian and Ahmadi \(1998\)](#), [Sturm and Hofmann \(2009\)](#), [Sturm \(2014\)](#), [Sturm \(2017\)](#). Results can be useful to calculate filtration efficiency of lung with respect to other shaped nonspherical nanoparticles. Although, in the

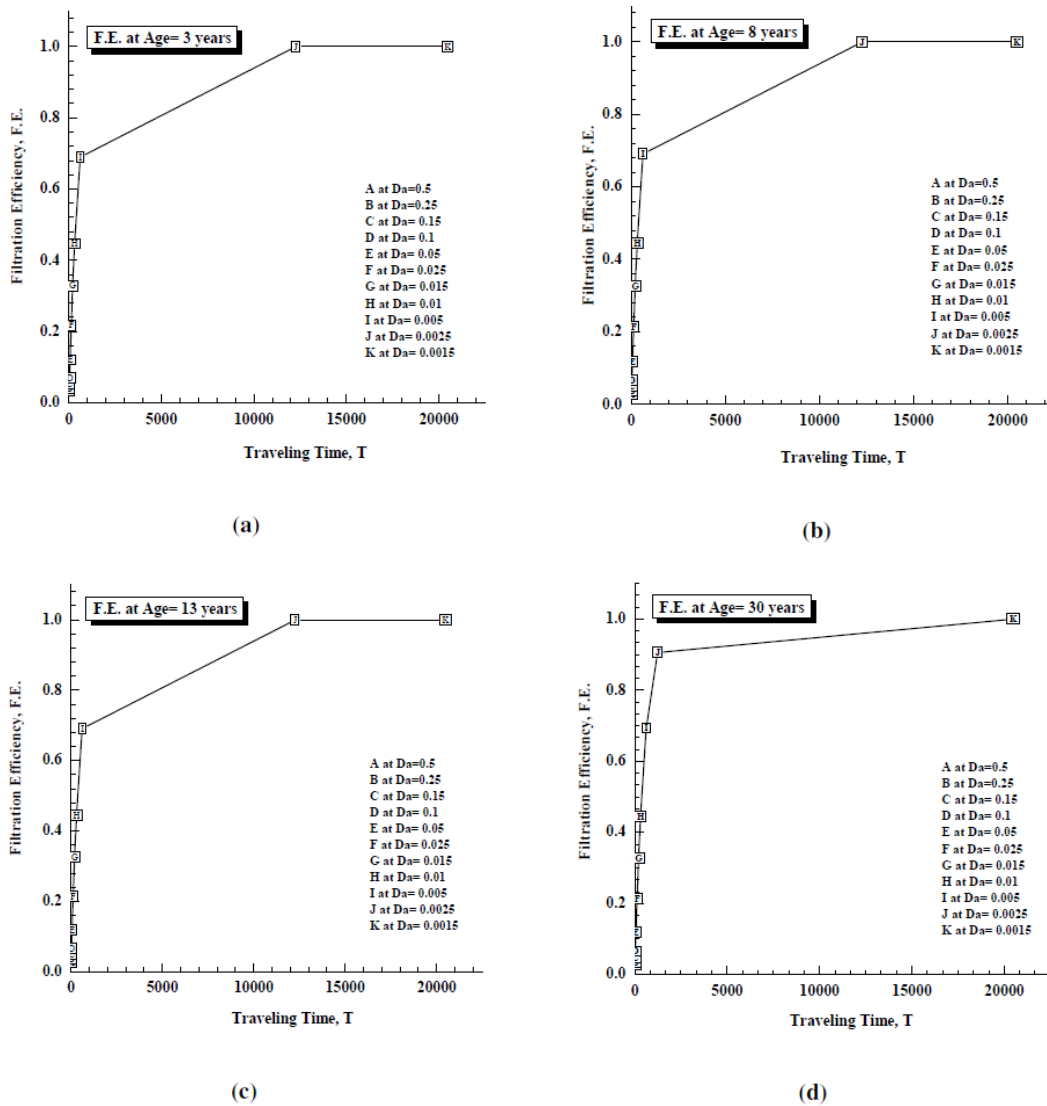


Fig. 8. Traveling time dependent filtration efficiency of lung at $\beta = 10$, $d=50\text{mm}$, $10^{-1} \leq Da \leq 10^{-3}$ (a) Situation at the age of 3 (b) (a) Situation at the age of 8 (c) Situation at the age of 13 (d) Situation at the age of 30.

Table 4 Correlation between traveling time (T) and filtration efficiency (F.E.) of lung from age 3-30

Darcy Number	Age=3		Age=8		Age=13		Age=30	
	T	F.E.	T	F.E.	T	F.E.	T	F.E.
0.5	17.5439	0.0328	14.3885	0.027	14.0845	0.0264	14.0845	0.0264
0.25	21.2766	0.0396	19.2308	0.0359	18.8679	0.0352	18.8679	0.0352
0.15	28.86	0.0534	26.2467	0.0486	26.0078	0.0482	26.0078	0.0482
0.1	37.9507	0.0696	35.7143	0.0656	35.461	0.0652	35.461	0.0652
0.05	67.5676	0.1205	66.0066	0.1179	66.0066	0.1179	66.0066	0.1179
0.025	129.0323	0.2174	127.3885	0.215	126.58237	0.2138	126.5823	0.2138
0.015	209.6436	0.3286	207.9002	0.3263	207.9002	0.3263	207.9002	0.3263
0.01	311.042	0.4462	309.5975	0.4447	309.5975	0.4447	309.5975	0.4447
0.005	615.3846	0.6894	617.284	0.6905	617.284	0.6905	623.053	0.6939
0.0025	12270	1	12270	1	12270	1	1242.2	0.9056
0.0015	20492	1	20492	1	20492	1	20492	1

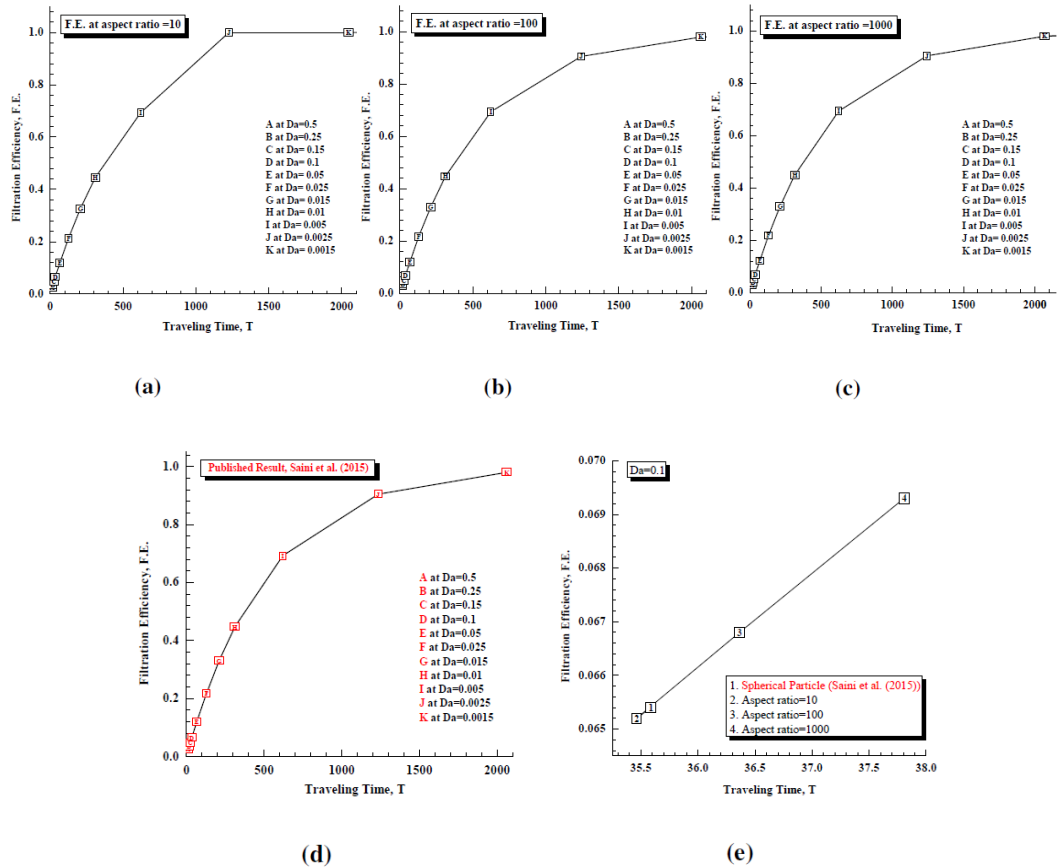


Fig. 9. Traveling time dependent filtration efficiency of spherical and nonspherical (10b1000) nanoparticle at age=15, $10^{-1} \leq Da \leq 10^{-3}$ (a) Situation for $\beta=10$ (b) Situation for $b=100$ (c) Situation for $b=1000$ (d) Situation for spherical particle (e) Comparison between F.E. of spherical and nonspherical nanoparticle at $Da=0.1$.

Table 5 Traveling time (t) and filtration efficiency (F.E.) of lung for different shape particles at the age of 15 and $10^{-1} \leq Da \leq 10^{-3}$

Darcy Number	Spherical Particle (Saini et al. (2015))		Aspect Ratio=100		Aspect Ratio=1000		Aspect Ratio=10	
	t	F.E.	t	F.E.	t	F.E.	t	F.E.
0.5	13.4228	0.0252	14.0845	0.0264	14.7059	0.0276	15.748	0.0295
0.25	18.3486	0.0343	18.8679	0.0352	19.6078	0.0366	20.8333	0.0388
0.15	25.7069	0.0477	26.0078	0.0482	26.738	0.0495	28.1294	0.052
0.1	35.5872	0.0654	35.461	0.0652	36.3636	0.0668	37.8072	0.0693
0.05	67.3401	0.1201	66.0066	0.1179	67.1141	0.1197	68.7285	0.1224
0.025	129.0323	0.2174	126.5823	0.2138	128.2051	0.2162	129.8701	0.2187
0.015	210.5263	0.3297	207.9002	0.3263	209.8636	0.3288	211.6402	0.3311
0.01	312.5	0.4477	309.5975	0.4447	312.0125	0.4472	314.4654	0.4498
0.005	621.118	0.6928	621.118	0.6928	623.053	0.6939	623.053	0.6939
0.0025	1234.6	0.9042	1227.0	1	1242.2	0.9056	1242.2	0.9056
0.0015	2061.9	0.9801	2049.2	1	2064	0.9802	2070.4	0.9804

present investigation we have considered one dimensional flow of air, but it can be extended for two to three dimensional flow and simultaneous changes can be done in the present model.

ACKNOWLEDGMENT

The author, Jyoti Kori, is thankful to Ministry of Human Resource Development India (Grant Code:-MHR-02-23-200-44) for providing fund and support while writing this manuscript.

REFERENCES

Aitken, R, K. S. Creely and T. Lang (2004). Nanoparticle: An Occupational Hygiene Review. *Institute of Occupational Medicine for the Health and Safety Executive*, 1-102.
 Alison, H. and R. Lynne (1974). Development of the acinus in the human lung. *Thorax* 29(1), 90-94.
 Asgharian, B. and G. Ahmadi (1998). Effect of fiber

- geometry on deposition in small air-ways of the lung. *Aerosol Science and Technology* 4, 59–474.
- Behnke, M., W. Kreyling, H. Schulz, S. Takenaka, J. P. Butler, F. Henry and A. Tsuda (2012). Nanoparticle delivery in infant lungs. *PNAS* 109(13), 50925097.
- Chitwood, D. and J. Devinny (1999). Evaluation of a two-stage biofilter for treatment of potw waste air. *Environ Prog* 18, 21222.
- Davies, G. and L. Reid (1970). Growth of the alveoli and pulmonary arteries in childhood. *Thorax* 25, 669.
- DeGroot, C. and A. Straatman (2018). A porous media model of alveolar duct flow in the human lung. *Journal of Porous Media* 21, 405–422.
- Dunnill, M. S. (1962). *Postnatal growth of the lung*. Thorax.
- Emery, J. and A. Mithal (1960). The number of alveoli in the terminal respiratory unit of man during late intrauterine life and childhood. *Archives of Disease in Childhood* 35, 544–7.
- Ergun, S. (1952). Fluid flow through packed columns. *Chemical Engineering Process* 48, 89–94.
- Henry, F. and A. Tsuda (2016). Onset of alveolar recirculation in the developing lungs and its consequence on nanoparticle deposition in the pulmonary acinus. *Journal of Applied Physiology* 120, 3854.
- Hinds, W. (1999). *Aerosol technology: properties, behavior, and measurement of airborne particles*. Wiley, New York.
- Hodge, D. and J. Devinny (1995). Modeling removal of air contaminants by biofiltration. *Journal of Environmental Management* 121(1), 21–44.
- Hofmann, W. (1982). Mathematical model for the postnatal growth of the human lung. *Respiration Physiology* 49, 115–129.
- Hogberg, S., H. Akerstedt, T. Lundstrom and J. Freund (2010). Respiratory Deposition of Fibers in the Non-Inertial Regime-Development and Application of a Semi-Analytical Model. *Aerosol science and technology* 44, 847–860.
- Jiang, Q., Z. Zhang and Y. W. Wang (2000). Thermal stability of low dimensional crystals. *Materials Science And Engineering A-Structural Materials* 286(1), 139–143.
- Kim, J., R. Heise, A. Reynolds and R. Pidaparti (2017). Aging effects on airflow dynamics and lung function in human bronchioles. *Aging effects on airflow dynamics and lung function in human bronchioles* 12(8), e0183654.
- Kori, J. and Pratibha (2018). Numerical simulation of mucus clearance inside lung airways. *Journal of Applied Fluid Mechanics* 11(5), 1163–1171.
- Laurent, S., D. Forge, M. Port, A. Roch, C. Robic, L. V. Elst and R. Muller (2010). Magnetic iron oxide nanoparticles: synthesis, stabilization, vectorization, physicochemical characterizations, and biological applications. *Chemical Reviews* 110(2574-2574).
- Menache, M. G. and R. C. Graham (1997). Conducting airway geometry as a function of age. *Annals of Occupational Hygiene* 41, 531.
- Nanda, K., S. Sahu and S. Behera (2002). Liquid-drop model for the size-dependent melting of low-dimensional systems. *Physical Review A* 66(1), 13208.
- Ochs, M., J. Nyengaard, A. Jung, L. Knudsen, M. Voigt, T. Wahlers, J. R., H. Jrgen and G. Gundersen (2004). The number of alveoli in the human lung. *American Journal of Respiratory and Critical Care Medicine* 169, 120124.
- Pozin, N. (2017). *Multiscale lung ventilation modeling in health and disease. Modeling and Simulation*. Ph. D. thesis, Paris 6.
- Qi, W., M. Wang and Q. H. Liu (2005). Shape factor of nonspherical nanoparticles. *Journal of Materials Science* 40, 27372739.
- Quirk, J., A. Sukstanskii, J. Woods, B. Lutey, M. Conradi, D. Gierada, R. Yusem, M. Castro and D. Yablonskiy (2016). Experimental evidence of age-related adaptive changes in human acinar airways. *Journal of Applied Physiology* 120(2), 159–165.
- Rissler, J., H. Nicklasson, A. Gudmundsson, P. Wollmer, E. Swietlicki and J. Lundahl (2017). A set-up for respiratory tract deposition efficiency measurements (15-5000 nm) and first results for a group of children and adults. *Aerosol and Air Quality Research* 17, 1244–1255.
- Roman, M., H. Rossiter and R. Casaburi (2016). Exercise, ageing and the lung. *European Respiratory Journal* 48(5), 1471–1486.
- Saini, A., V. K. Katiyar and Pratibha (2015). Numerical simulation of gas flow through a biofilter in lung tissues. *World Journal of Modelling and Simulation* 11(1), 33–42.
- Simakin, A., V. Voronov, G. Shafeev, R. Brayner and F. Bozon-Verduraz (2001). Nanodisks of Au and Ag produced by laser ablation in liquid environment. *Chemical Physics Letters* 348(3), 182–186.
- Smith, G. D. (1985). *Numerical Solution of Partial Differential Equations*. Oxford Univ. Press, Third Edition.
- Stober, W. (1972). *Dynamic shape factors of nonspherical aerosol particles. Assessment of Airborne Particles*, Charles C Thomas Publisher, Springfield, 249289.
- Sturm, R. (2014). Theoretical deposition of nanotubes in the respiratory tract of children and adults. *Annals of Translational Medicine*

- 2(1), 6.
- Sturm, R. (2015). A computer model for the simulation of nanoparticle deposition in the alveolar structures of the human lungs. *Annals of Translational Medicine* 3(19), 281.
- Sturm, R. (2016). Bioaerosols in the lungs of subjects with different ages-part 1: deposition modeling. *Annals of Translational Medicine* 4(11), 211.
- Sturm, R. (2017). Bioaerosols in the lungs of subjects with different ages-part 2: clearance modeling. *Annals of Translational Medicine* 5(5), 95.
- Sturm, R. and W. Hofmann (2009). A theoretical approach to the deposition and clearance of fibers with variable size in the human respiratory tract. *Journal of Hazardous Materials* 170, 210–218.
- Svartengren, M., R. Falk and K. Philipson (2005). Long-term clearance from small air-ways decreases with age. *European Respiratory Journal* 26, 609615.
- Tiwari, J., R. Tiwari and K. Kim (2012). Zero-dimensional, onedimensional, two-dimensional and three-dimensional nanostructured materials for advanced electrochemical energy devices. *Progress in Materials Science* 57, 724803.
- Weibel, E. (1963). *Morphometry of the Human Lung*. Springer-Verlag Berlin Heidelberg.
- Xu, G. and C. Yu (1986). Effects of age on deposition of inhaled aerosols in the human lung. *Aerosol Science and Technology* 5(3), 349–357.
- Yan, W., Y. Liu, Y. Xu and X. Yang (2008). Numerical simulation of air flow through a biofilter with heterogeneous porous media. *Bioresource Technology* 99, 1562161.
- Yan, W., Z. Su and H. Zhang (2013). Effect of non-isothermal condition on heterogeneous flow through biofilter media by lattice boltzmann simulation. *Journal of Chemical Technology & Biotechnology* 88, 456–461.